RAPID COMMUNICATIONS

PHYSICAL REVIEW B VOLUME 41, NUMBER 5 15 FEBRUARY 1990-I

Differential absorption spectroscopy of charge distributions in double-barrier tunnel structures

I. Bar-Joseph,* T. K. Woodward, and D. S. Chemla
AT&T Bell Laboratories, Holmdel, New Jersey 07733

D. Sivco and A. Y. Cho
AT&T Bell Laboratories, Murray Hill, New Jersey 07974

(Received 14 August 1989; revised manuscript received 29 November 1989)

Differential absorption spectroscopy is used to determine the charge density in $In_xGa_{1-x}As/In_xAl_{1-x}As$ double-barrier tunneling structures. We show the formation of accumulation and depletion regions on either side of the double barrier, and measure with an absolute calibration the accumulated charge in the 45-Å quantum-well region of the structures. Peak charge densities $\approx 5.4\times10^{10}$ cm^{-2} and $\approx 3.9\times10^{10}$ cm^{-2} are measured for barrier thicknesses of 70 and 56 Å, respectively. The corresponding calculated transit times are 70 and 20 ps.

The phenomenon of tunneling is one of the most fundamental predictions of quantum mechanics. Its manifestations in the α decay of the nucleus and tunneling microscopy are probably the most widely known. Epitaxial crystal-growth techniques have enabled the tailoring of the potential inside a semiconductor heterostructure to a few atomic layers. This has set the stage for an active experimental and theoretical field concerned both with testing the fundamental concepts of tunneling and constructing devices based on such concepts. The double-barrier diode (DBD) is a device that has generated interest on both counts. Substantial progress has been made since the first observation of tunneling in DBD's,[1] with remarkable improvement in the quality of the negative differential resistance (NDR), demonstration of high-frequency operation, and the development of sophisticated devices.[2] Nevertheless, some of the most basic questions related to the operating principles remain to be settled. These issues include the question of tunneling time, the amount of charge stored in the well, the existence of intrinsic bistability, as well as the characterization of the process as sequential or coherent.[3-7] Differential absorption spectroscopy can address all these issues by determining the amount of charge accumulated in the well during the operation of the DBD.[8] This point was recently addressed in photoluminescence (PL) experiments, wherein PL intensity was correlated with the current through the diode.[9] This behavior was interpreted as an indication of charge storage and values for the electron density and tunneling times were deduced.

A more direct method, which is better suited for a quantitative evaluation of electron density in semiconductor structures, is differential absorption spectroscopy (DAS). This technique monitors changes in the absorption spectrum due to the presence of carriers or fields. Its strength lies in the fact that absorption in semiconductors reflects intrinsic processes, whose cross section can be determined *experimentally very accurately*. Furthermore, it is relatively insensitive to the presence of impurities, defects, etc. There exists, therefore, an intrinsic calibration to which the measured absorption changes can be compared, which is not the case with PL.[10] Moreover, the spectral resolution of this technique provides information about electronic states other than the lowest-energy ones, and in the case of DBD, about the contact layers as well. In the case of quantum wells (QW), screening is negligible as compared to the effects of Pauli exclusion,[11] and the occupation of electron or hole states produce bleaching of the absorption that is well understood[12] and quantified.[13] Recently, DAS has been shown to be a very sensitive and quantitative probe of electron density and field inside the QW-conducting channel of modulation-doped field-effect transistors (MOD-FET).[14,15] It has provided detailed information over a very broad spectral range and about electronic states at various energies.

In this paper we report the application of DAS to DBD's. We determine the charge distribution across the structure, and get absolute values for the electron density inside the well. We show that DAS is an excellent tool for characterization of QW transport devices.

Measurements were performed on two molecular-beam epitaxy (MBE) grown samples. The general structure is shown in the inset of Fig. 1. The DBD consists of 56-Å barriers in sample *A* and 70 Å in sample *B*. The well size is 45 Å in both samples. (These values are determined by TEM measurements on sample *B*.) The samples were processed to form mesas of different sizes and were antireflection coated. The measurements reported in this paper were done on 150-μm^2 mesas. The diodes show a profound NDR behavior. The peak-to-valley current ratio at room temperature is about 4, and 20 is seen at 10 K.

For optical measurements the samples were mounted on sapphire windows on a cold finger of a continuous-flow helitran and held at a temperature of about 10 K. Light from a 100-W tungsten bulb was passed through a spectrometer and imaged on the sample to form a 100×100-μm spot. The incident intensity was very weak and had no measurable effect on the *I-V* curve. The voltage on the device was modulated at 470 Hz between 0 and V_{max} with a square wave, and the transmitted light was detected using conventional lock-in techniques. In Fig. 2 we show three DAS spectra taken at three values of V_{max}. The dotted spectrum was taken at low voltage, wherein the diode is biased but there is a negligible current. The solid spec-

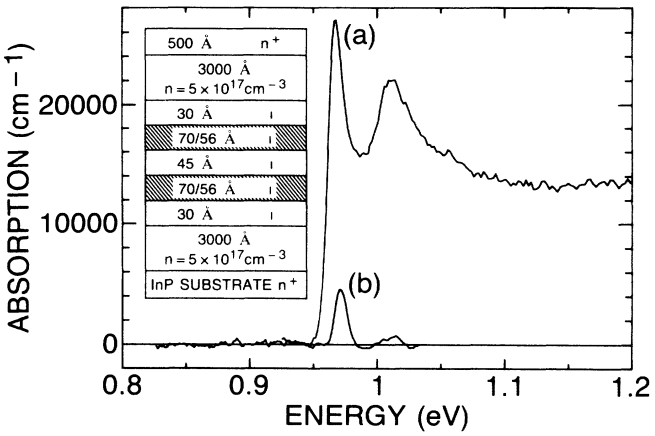

FIG. 1. (a) Absorption spectrum for a sample consisting of 50 periods of 70 Å of $In_{0.52}Al_{0.48}As$ barriers and 45 Å of $In_{0.53}Ga_{0.47}As$ quantum well grown in the same conditions as sample *B*, normalized to the total $In_{0.53}Ga_{0.47}As$ thickness. (b) QW contribution to the differential absorption spectrum of the DBD for the peak current of sample *B*. Inset: Sample structure, shaded region corresponds to $In_{0.52}Al_{0.48}As$, other regions to $In_{0.53}Ga_{0.47}As$.

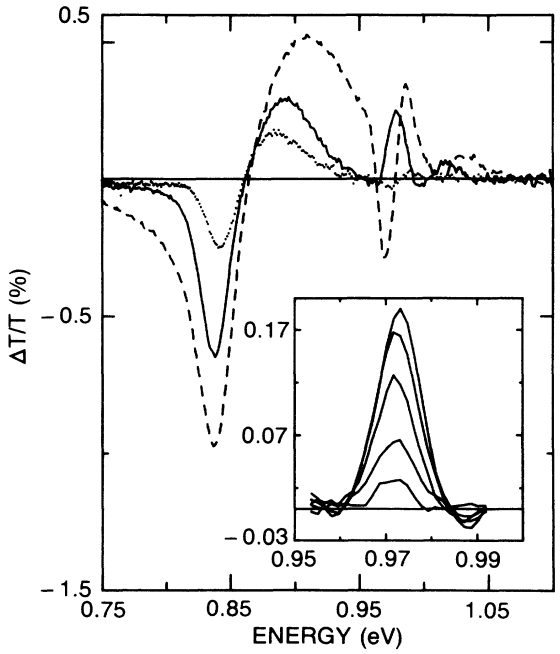

FIG. 2. DAS spectra for sample *B*, at 10 K, for low current (dotted line), peak current (solid line), and valley current (dashed line). Inset: Blow up of the heavy-hole signal for various currents between the onset of tunneling and the peak of the NDR (see Table I).

trum corresponds to the peak of the NDR characteristic at which the current is large. The voltage for the dashed spectrum is past the peak of the NDR and the current is low.

Three distinct spectral regions are clearly identified in Fig. 2. From low to high energies one sees a negative peak around 0.83 eV, a positive peak around 0.9 eV, and some narrow features near 0.97 eV. In order to have an unambiguous assignment of the origin of these spectral features we have grown under exactly the same calibrations a 50 period reference multiple QW sample with the same barrier and well widths as in sample *B*. The measured absorption spectrum is shown in Fig. 1. We have also measured the absorption of thick $In_xGa_{1-x}As$ layers. The narrow DAS features at 0.97 and 1.0 eV correspond to the heavy-hole (hh) and light-hole (lh) peaks of the QW. The onset of the negative peak, around 0.8 eV, is at the gap of the bulk $In_xGa_{1-x}As$, E_g, and the crossover between the positive and negative lobes is at about E_g+E_f, where $E_f \approx 55$ meV is the Fermi energy in this sample. We therefore attribute the signals at energies larger than 0.940 eV to the QW of the DBD, and the low-energy ones to absorption changes in the contact layers.

We shall first discuss the two QW related features, which lie between 1.01 and 0.95 eV. Their energies agree well with the position of the hh and lh excitons measured on the multiple QW sample, as seen in Fig. 1. The energy of the lower feature also agrees well (within 2 meV) with the calculated hh-exciton transition. The agreement with the calculated lh transition for the higher-energy feature is less satisfactory (16-mV discrepancy). A possible explanation is that because the lh exciton lies in the hh continuum for this narrow QW, Fano interference effects distort its shape and shift the position of the peak as compared to the value calculated from simple theory. The lh signal is ≈ 4 times weaker than that of the hh. Since both the hh and the lh signals represent transitions to the same conduction-band states, this is explained by the difference in their oscillator strengths. We shall focus in the following on the hh signal. When V_{max} is small the hh DAS has a small differential-shape profile, characterized by a positive peak followed by a negative one of approximately the same size (dotted line of Fig. 2). At higher voltages, it changes to a positive peak with a maximum of 0.972 eV (solid line). This regime is magnified in the inset of Fig. 2. As V_{max} increases beyond the switching voltage the line shape changes abruptly to a strong differential signal (dashed line).

There is a clear difference between a *voltage* related DAS and a *charge* related one. A voltage drop on a QW causes a shift of the excitonic absorption edge due to the quantum confined Stark effect[16] and therefore yields a differential shaped DAS. Charge accumulation (or depletion) on the other hand yields a positive (or negative) transmission change ΔT because of the inhibition (or allowance) of optical transitions due to the Pauli exclusion principle[15] (phase-space filling and exchange interaction[13]). We can therefore conclude that the signals at low and high voltages represent the large electric-field drop in the well ($\approx 1.4\times10^5$ V/cm when the diode is biased just above the switching point) with *no* charge accumulation. At the intermediate voltages, the signals of both the hh and the lh excitons are positive and therefore represent *charge accumulation* in the well. The abrupt change of the DAS line shape as V_{max} crosses V_{peak} demonstrates the sudden decrease of the charge in the QW. In the high-voltage regime, however, the signal coming from the con-

TABLE I. Summary of results for the two samples.

Sample *B*			Sample *A*		
J (A/cm^2)	$\Delta T/T_0$	N (10^{10} cm^{-2})	J (A/cm^2)	$\Delta T/T_0$	N (10^{10} cm^{-2})
23	2.7×10^{-4}	0.8	102	3.6×10^{-4}	1.1
43	6.2×10^{-4}	1.8	191	9.4×10^{-4}	2.8
65	1.2×10^{-3}	3.6	280	1.3×10^{-3}	3.9
86	1.6×10^{-3}	4.8	321	1.3×10^{-3}	3.9
121	1.8×10^{-3}	5.4			

tact layers extends to higher energies and interferes with the QW signal. This regime requires a careful analysis and will be discussed in a forthcoming publication. Experiments performed with sample *B* (thicker barriers) give results that are qualitatively very similar to those obtained on sample *A*. The only qualitative difference is that the hh and lh peaks are larger in *B*. This implies that the charge stored in the well with the thicker barrier is larger.

To evaluate the electron density N in the QW we use the analysis developed to explain QW absorption saturation experiments[12,13] and already applied successfully to MOD-FET's.[14,15] As electrons populate the first resonance level their presence inhibits exciton formation by blocking states from participating in the wave function, and also by Coulomb effects (screening), which in quantum wells is mainly due to the exchange interaction.[13] In the limit of low density the change Δf of the exciton oscillator strength f is $\Delta f/f = N/N_s$, where N_s is the exciton saturation density, a saturation parameter that is related to the square of the two-dimensional Bohr radius.[13] Since $\Delta f/f = \Delta\alpha/\alpha$ we can relate N to $\Delta\alpha$. It is clear that an exact determination of N_s is critical to obtain an accurate value for N. We therefore performed a careful low-temperature (10 K) measurement of this parameter on the QW reference sample. We measured, with a pump-probe technique, both the relaxation time and the saturation intensity, which were used to determine the number of carriers deposited in the sample, N. Obtaining the absorption bleaching $\Delta\alpha$ with a $\Delta T/T$ measurement, and knowing α (Fig. 1), we use $\Delta\alpha/\alpha = N/N_s$ to obtain $N_s = 2.7\times10^{11}$ cm^{-2}. This value is in reasonable agreement with both the low-temperature theoretical value for $In_xGa_{1-x}As$ QW's (Ref. 13) of $N_s \approx 1.5\times10^{11}$ cm^{-2}, and with the room-temperature data[17] of $N_s = 1.5\times10^{11}$ cm^{-2}. Using our measured value for N_s and the measured absorption for the hh exciton peak we deduce the charge in the QW for the various current densities shown in Table I. The small relative change in the absorption caused by the stored charge is shown in Fig. 1, where it is superimposed on the reference sample absorption spectrum. The reason for the low charge storage is that in a symmetric structure under bias the rate for tunneling out of the well is much larger than the rate for tunneling in.[18] It can therefore be expected that larger charge accumulation would exist in asymmetric structures.

From the measured current and charge densities one can deduce a transit time through the double-barrier structure given by $\tau = Ne/J$. In the case of peak charge accumulation we get $\tau = 72$ ps for sample *B* and $\tau = 20$ ps for sample *A*. Experimental uncertainty as to the precise value of J to use for a given value of N can account for some nonmonotonic variation in τ for other entries in Table I, since J is obtained from a separately measured *I-V* curve. There may also be bias dependence to the transit time that is masked by this uncertainty. In the coherent model this transit time is related to the width of the transmission resonance by $\tau = \hbar/\Delta E$. The corresponding calculated values for $\hbar/\Delta E$ in a biased structure depend strongly on the shape of the potential, particularly the conduction-band offset ΔE_c and the details of the model used. For example, using a transfer-matrix approach,[19] we obtain 50 ps $< \tau <$ 140 ps for sample *B* and 8 ps $< \tau <$ 20 ps for sample *A* when 0.41 eV $< \Delta E_c <$ 0.49 eV. The transit times deduced from the charge measurements are therefore in qualitative agreement with the coherent tunneling model.

Let us consider now the signal which originates from the contact layers. Figures 3(a) and 3(b) illustrate the potential diagrams versus the coordinate perpendicular to the DBD, x, for $V = 0$ and $V = V_{max}$. Under bias an accumulation layer forms on the left-hand side of the double barrier, while depletion occurs on the other side. The difference between the quasi Fermi level and the bottom

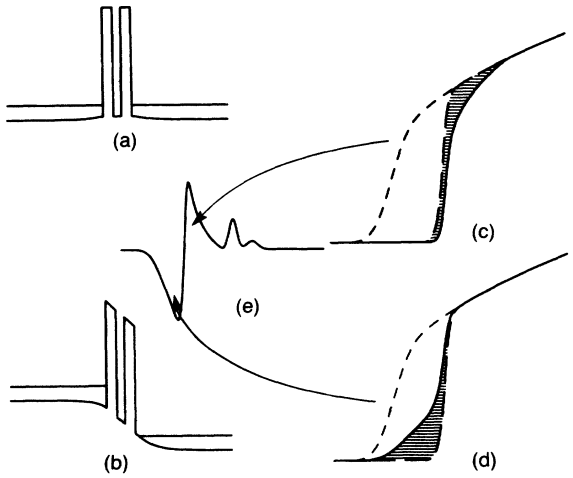

FIG. 3. Schematic explanation of the origin of the DAS signals in the accumulation and depletion layers: (a) and (b) band diagrams without and with bias, respectively, (c) and (d) absorption profile in the accumulation and depletion layers, respectively, and (e) schematic of the DAS.

of the conduction band $\Delta(x) = E_F - E_c(x)$ is thus a function of x. The signal measured in a DAS experiment is

$$\frac{\Delta T}{T_0} = \int dx \{\exp[\alpha(x, V=0) - \alpha(x, V=V_{\max})] - 1\}, \quad (1)$$

where $\alpha(x, V=0)$ and $\alpha(x, V=V_{\max})$ are the absorption coefficients at x with zero and applied bias. The absorption profile of the undoped bulk material $\alpha(x, V=0)$, which is schematically shown by the short-dashed line in Figs. 3(c) and 3(d), starts at E_g. At zero bias, the optical absorption in the cladding layers can only occur for photon energy $> E_g + E_f$, and its profile is shown by the long-dashed line in Figs. 3(c) and 3(d). In the accumulation region, the quasi Fermi level is effectively pushed higher into the band. The sample is thus slightly more transparent at energies between $E_g + E_f$ and $E_g + \Delta(x)$. The edge of the integrated absorption on the left-hand side of the double barrier, which is shown by the solid line in Fig. 3(c), is moved to higher energies. The difference between the absorption spectra for $V=0$ and $V=V_{\max}$ yields a positive DAS signal just above $E_g + E_f$ as illustrated in Fig. 3(e). Conversely, in the depletion region, absorption onsets at E_g, and the sample is slightly more opaque at energies between E_g and $E_g + E_f$. The integrated absorption in this layer is shown by the solid line in Fig. 3(d). The difference of the absorption spectra in the depletion layer gives a negative DAS-signal just below $E_g + E_f$ and extends to E_g. With this explanation, we understand both the sign and the position of these peaks. We note that Fig. 3(e) shows a rather symmetric line shape whereas we observe a much larger signal coming from the depletion layer. The strength of the DAS signal is primarily related to the extent of a certain sheet density. This asymmetry might indicate that the accumulation layer is narrower than the depletion layer. This is a subject for further investigation.

In summary, we have reported the first application of the DAS technique to DBD's. Our results directly show the accumulation of charge in the QW for biases less than the peak of the NDR. A maximum charge density of 5.4×10^{10} cm^{-2} is estimated. This low density has a negligible effect on the potential profile across the DBD. Larger densities are expected in asymmetric structures. The DAS also unambiguously determines the presence of depletion and accumulation layers, whose width and charge distribution can be determined.[20] Transit time estimates obtained from our charge measurements and the $I(V)$ curves of the two devices yield 70 and 20 ps.

We warmly thank A. Ourmazd for the accurate determination of the thicknesses of the QW's by TEM lattice imaging, M. Wegener for his contribution to the nonlinear optical experiments, and D. A. B. Miller for the transfer-matrix program.

---

*Present address: Department of Physics, Weizmann Institute of Science, 76100 Rehovot, Israel.

[1] L. L. Chang, L. Esaki, and R. Tsu, Appl. Phys. Lett. **24**, 593 (1974).

[2] F. Capasso, S. Sen, F. Beltram, and A. Y. Cho, in *Integrated Circuits in the 0.5 to 0.05 μm Dimensional Range,* edited by R. K. Watts (Wiley, New York, 1989).

[3] N. S. Windgreen, K. W. Jacobson, and J. W. Wilkins, Phys. Rev. Lett. **61**, 1396 (1988); **61**, 2633(E) (1988).

[4] P. J. Price, Phys. Rev. B **36**, 1314 (1987).

[5] V. J. Goldman, D. C. Tsui, and J. E. Cunningham, Phys. Rev. Lett. **58**, 1256 (1987); **59**, 1632 (1987).

[6] S. Luryi, Appl. Phys. Lett. **47**, 490 (1985).

[7] T. Weil and B. Vinter, Appl. Phys. Lett. **50**, 1281 (1987).

[8] V. J. Goldman, D. C. Tsui, and J. E. Cunningham, Phys. Rev. B **35**, 9387 (1987).

[9] J. F. Young, B. M. Wood, G. C. Aers, R. L. S. Devine, H. C. Liu, D. Landheer, M. Buchanan, A. J. SpringThorpe, and P. Mandeville, Phys. Rev. Lett. **60**, 2085 (1988).

[10] W. R. Frensley, M. A. Reed, and J. H. Luscombe, Phys. Rev. Lett. **62**, 1207 (1989).

[11] S. Schmitt-Rink, D. S. Chemla, and D. A. B. Miller, Adv. Phys. **38**, 89 (1989).

[12] D. S. Chemla, D. A. B. Miller, P. W. Smith, A. C. Gossard, and W. Wiegmann, IEEE J. Quantum Electron. **QE-20**, 265 (1984).

[13] S. Schmitt-Rink, D. S. Chemla, and D. A. B. Miller, Phys. Rev. B **32**, 6601 (1985).

[14] I. Bar-Joseph, J. M. Kuo, C. Klingshirn, G. Livescu, Y. Y. Chang, D. A. B. Miller, and D. S. Chemla, Phys. Rev. Lett. **59**, 1357 (1987).

[15] D. S. Chemla, I. Bar-Joseph, J. M. Kuo, T. Y. Chang, C. Klingshirn, G. Livescu, and D. A. B. Miller, IEEE J. Quantum Electron. **QE-24**, 1664 (1988).

[16] D. A. B. Miller, D. S. Chemla, T. C. Damen, A. C. Gossard, W. Wiegmann, T. H. Wood, and C. A. Burrus, Phys. Rev. B **32**, 1043 (1985).

[17] J. Weiner and D. S. Chemla, Appl. Phys. Lett. **49**, 531 (1986).

[18] R. Ricco and M. Ya. Azbel, Phys. Rev. B **29**, 1970 (1984).

[19] R. Tsu and L. Esaki, Appl. Phys. Lett. **22**, 562 (1973).

[20] T. K. Woodward, I. Bar-Joseph, D. S. Chemla, D. Sivco, and A. Y. Cho (unpublished).